Form factors of the $d^*(2380)$ resonance

Yubing Dong,[1,2,3,*] Pengnian Shen,[4,1,2,†] and Zongye Zhang[1,2,3,‡]

[1]*Institute of High Energy Physics, Chinese Academy of Sciences, Beijing 100049, China*
[2]*Theoretical Physics Center for Science Facilities (TPCSF), CAS, Beijing 100049, China*
[3]*School of Physical Sciences, University of Chinese Academy of Sciences, Beijing 101408, China*
[4]*College of Physics and Technology, Guangxi Normal University, Guilin 541004, China*

(Received 16 January 2018; published 5 June 2018)

In order to explore the possible physical quantities for judging different structures of the newly observed resonance $d^*(2380)$, we study its electromagnetic form factors. In addition to the electric charge monopole $C0$, we calculate its electric quadrupole $E2$, magnetic dipole $M1$, and magnetic octupole $M3$ form factors on the base of the realistic coupled $\Delta\Delta + C_8C_8$ channel d^* wave function with both the S- and D-partial waves. The results show that the magnetic dipole moment and electric quadrupole deformation of d^* are 7.602 and 2.53×10^{-2} fm^2, respectively. The calculated magnetic dipole moment in the naive constituent quark model is also compared with the result of $D_{12}\pi$ picture. By comparing with partial results where the d^* state is considered with a single $\Delta\Delta$ and with a $D_{12}\pi$ structures, we find that in addition to the charge distribution of d^*, the magnetic dipole moment and magnetic radius can be used to discriminate different structures of d^*. Moreover, a quite small electric quadrupole deformation indicates that d^* is more inclined to a slightly oblate shape due to our compact hexaquark dominated structure of d^*.

DOI: 10.1103/PhysRevD.97.114002

I. INTRODUCTION

Since the dibaryon state was proposed more than 50 years ago, the existence of the dibaryon has become one of the hot topics in particle and nuclear physics. Among those states, H particle and d^* states were involved most. In particular, the d^* state has intensively been studied by various models from the hadronic degrees of freedom to the quark degrees of freedom more than half century. Its mass prediction was ranged from a few MeV to several hundred MeV. Searching such a state has also been considered as one of the aims in several experimental projects. However, no confidential results were released until 2009. Since then, a series of experimental studies for d^* was carried out in the study of ABC effect by CELSIUS/WASA and WASA@COSY Collaborations. [1–4]. Various double-pion and single-pion decays of d^*, including invariant mass spectra, Dalitz plots, Argon plots, in the pn and pA reactions, the analyzing power of the neutron-proton scattering and etc., have been carefully measured and analyzed. It was found that the results cannot be explained by the contribution either from the intermediate Roper excitation or from the t-channel $\Delta\Delta$ contribution, except introducing an intermediate new resonance. Then, the discovery of a new resonance with a mass of about 2370–2380 MeV, a width of about 70–80 MeV, and the quantum numbers of $I(J^P) = 0(3^+)$ was announced [1–4]. Since the baryon number of the resonance is 2, it is believed that such a state is just the d^* state which has been hunted for several decades, and, in general, can be explained by either "an exotic compact particle" or "a hadronic molecule state."

It should be emphasized that the threshold (or cusp) effect may not be so significant in the d^* case as that in the XYZ particle case due to the fact that the observed mass of d^* is about 80 MeV below the $\Delta\Delta$ threshold and about 70 MeV above the $\Delta\pi N$ threshold [5–7]. In addition, if d^* does exist, it contains at least 6 light quarks, and it is also different from the XYZ particles which contain heavy flavor.

Following the reports of Refs. [1–4], many theoretical models for the structure of d^* have been developed or proposed. Up to now, there are mainly two structural schemes which attract considerable attention of physicists. One of them assumes that the d^* state has a compact structure, and may be an exotic hexaquark dominated state whose mass is about 2380–2414 MeV and width about 71 MeV, respectively [8–15]. The other one, in order to explain the upper limit of the single-pion decay width of d^* [16], proposes that the d^* state is basically a molecular-like hadronic state with a $\alpha[\Delta\Delta] + (1-\alpha)[D_{12}\pi]$ mixing structure ($\alpha = 5/7$) [17], which originates from a three-body

*dongyb@ihep.ac.cn
†shenpn@ihep.ac.cn
‡zhangzy@ihep.ac.cn

$\Delta N\pi$ resonance assumption, where the pole position of the resonance locates around $(2363 \pm 20)+i(65 \pm 17)$ MeV [18,19], and a $D_{12}\pi$ molecular-like model, where the mass and width of the resonance are pre-fixed to be 2370 MeV and 70 MeV, respectively [20]. Although the experimental data can be explained by using either scheme, the described structures of d^* are quite different. Therefore, it is necessary to seek other physical observables which would have distinct values for different interpretations so that with the corresponding experimental data one would be able to justify which one is more reasonable.

It is well known that with the help of the electromagnetic probe, electromagnetic form factors become indispensable physical quantities in revealing the internal structure of a complicated system. For example, the electromagnetic form factors of a nucleon provide us the charge and magnetic distributions inside the nucleon. This fact exhibits the structure of the nucleon where a three quark core is surround by the pion cloud. It also tells that the charge and magnetic radii of the nucleon can be extracted by the slopes of the charge and magnetic distributions of the nucleon at $Q = 0$ (with Q being the momentum transfer) Refs. [21–24]. The accurately measured charge radius of the proton does justify the structure of the nucleon. Furthermore, in a spin-1 system, for instance a deuteron or a vector ρ-meson, the charge, magnetic and quadrupole form factors can also reveal its intrinsic structures, such as its charge and magnetic distributions and the quadrupole deformation (see, for example, Refs. [25–31] for the deuteron and Refs. [32–38] for the ρ meson, respectively). Consequently, the electromagnetic form factors might also be discriminating quantities for studying the inner structure of the higher spin particle. In particular, for the d^* state, if there is a considerably large hidden color component (HCC) in it, we found that, although such a component does not contribute to its hadronic strong decay in the leading-order calculation, it can play a rather important role in the charge distribution calculation [12–14,39]. The resultant charge distribution of d^* with a compact 6-quark structure is quite different from that having a $D_{12}\pi$ (or $\Delta\pi N$) structure [39]. Therefore, we believe that the charge distribution of d^* can serve as one of the criteria for judging its structure.

In general, a spin-3 particle has $2S + 1 = 7$ electromagnetic form factors, $C0$ (charge monopole form factor), $C2$ (or $E2$, electric quadrupole form factor), $C4$, and $C8$ for electric form factors and $M1$, $M3$, and $M5$ for magnetic form factors. Therefore, in order to understand the structure of d^*, the spin-3 particle, except the charge distribution (namely, the charge monopole form factor $C0$) calculated in our previous paper [39], we are going to study the other lower rank form factors of d^*, such as its electric quadrupole $E2$, magnetic dipole $M1$, and magnetic octupole $M3$ form factors, with a compact $\Delta\Delta + C_8C_8$ coupled-channel structure on the base of our chiral SU(3) constituent quark model.

In our previous studies [8,10–15], we enlarged the Fock space to involve the next lowest QCD allowed configuration, proposed the possible structure of d^* as a hexaquark dominated state and dynamically calculated it in the framework of the resonating group method (RGM) with a trial wave function of the $\Delta\Delta + C_8C_8$ structure in the chiral SU(3) constituent quark model. It should be stressed that the approach can explain most of the data available on the masses of the ground states of baryons, the scattering and reaction data of the baryon-baryon interactions, the binding energy of the deuteron and even H particle, etc. [40–44]. In this way, we obtained the mass and corresponding wave function of d^* with the proposed structure (refer to the Appendix for detail), and consequently, the partial widths in various double pion and single pion decay channels. All these calculated results consist with the data measured by the CELSIUS/WASA and WASA@COSY Collaborations. Therefore, in terms of resultant wave function, it is reasonable and possible to investigate some new observables for distinguishing the structure of d^*, and consequently to provide relevant predictions for reference in the future experimental observation.

This paper is organized as follows. In Sec. II, the wave function of d^* in the chiral SU(3) constituent quark model is briefly introduced. Section III is devoted to the electromagnetic form factors and the multipole decomposition of the electromagnetic current of the d^* resonance. Our numerical results and a short summary will be presented in Sec. IV.

II. WAVE FUNCTIONS OF $d^*(2380)$ IN CHIRAL CONSTITUENT QUARK MODEL

In studying possible dibaryons in 1999, a $\Delta\Delta + C_8C_8$ structure of the d^* state with $(I(J^P)) = (0(3^+))$, where I, J, P are isospin, spin, and parity, respectively, was firstly proposed [8]. With the assumption of such a structure, its mass was predicted [8]. In recent years, a series of sophisticated studies on the structure and decay properties of d^* has further been performed, and a compact picture for it, an exotic hexaquark dominated state, was deduced [8,10–14,39]. In order to get a meaningful result for a 6-quark system, those calculations were dynamically carried out on the quark degrees of freedom by using a chiral SU(3) constituent quark model. In this strong interaction model, the effective quark-quark interaction induced by the exchange of the chiral fields receives the contributions from the pseudoscalar, scalar, and vector chiral fields, respectively (see the Appendix). The model parameters are determined in such a way that the stability condition and the properties of nucleon, the mass splitting between the nucleon and Δ, the most masses of the ground states of baryons, the static properties of deuteron, and the phase shifts of the nucleon-nucleon scattering can be ensured. With these prefixed model parameters, we believe that the model has considerable prediction power [40,41].

In the practical calculation for d^*, we use the well-established resonating group method which has frequently been applied to the studies of nuclear physics and hadronic physics, especially where the clustering phenomenon exists [45–52]. In the RGM framework, if we assume again that the d^* state has a $\Delta\Delta + C_8C_8$ structure, the full 6-quark wave function reads

$$\Psi_{6q} = \mathcal{A}\Big[\hat{\phi}^A_\Delta(\vec{\xi}_1,\vec{\xi}_2,\mu^A_\Delta)\hat{\phi}^B_\Delta(\vec{\xi}_4,\vec{\xi}_5,\mu^B_\Delta)\eta_{\Delta\Delta}(\vec{r}) + \hat{\phi}^A_{C_8}(\vec{\xi}_1,\vec{\xi}_2,\mu^A_{C_8})\hat{\phi}^B_{C_8}(\vec{\xi}_4,\vec{\xi}_5,\mu^B_{C_8})\eta_{C_8C_8}(\vec{r})\Big]^{C=(00)}_{S=3,T=0}, \tag{1}$$

where S, T, and C represent the quantum numbers of the spin, isospin, and color, $\mathcal{A} = 1 - \sum_{i(\in A),j(\in B)} P^{OSFC}_{ij}$ is the total antisymmetrization operator, P^{OSFC}_{ij} denotes the exchange operator which exchanges the ith quark belonging to the cluster A and jth quark pertaining to the cluster B in the orbital, spin, flavor, and color spaces, $\hat{\phi}^{A(B)}_{\Delta(C_8)}$ is the antisymmetrized internal wave function of the (123)(or (456)) quark cluster A(or B) for $\Delta(C_8)$ with $\vec{\xi}_i$ [$i = 1, 2$ (4,5)] being its internal Jacobi coordinates and $\mu^{A(\mathrm{orB})}_{\Delta(C_8)}$ being an aggregate of the quantum numbers of the spin, isospin, and color of the $\Delta(C_8)$ cluster named A(or B) with $[S, I, C]_{\Delta(C_8)} = [3/2, 3/2, (00)((3/2, 1/2, (11)))]$ for the $\Delta(C_8)$ cluster, and the meanings of other symbols can be found in the Appendix. Clearly, C_8 stands for a colored cluster, and C_8C_8 represents hidden color channel. $\eta_{\Delta\Delta(C_8C_8)}$ is the relative wave function between A and B clusters which will be determined by dynamically solving the RGM equation [10,11]

$$\langle\delta\Psi_{6q}|H - E|\Psi_{6q}\rangle = 0 \tag{2}$$

of the system with the (extended) chiral SU(3) constituent quark model.

However, the resultant two components in Eq. (1) are not orthogonal to each other. In order to make them orthogonal to each other and to make the calculations simplified and feasible without missing most of the important effect of the antisymmetrization, we effectively rewrite Eq. (1) as an effective wave function in Eq. (3) in terms of channel wave function which was often employed in nuclear physics and hadronization in hadron physics [53–55]. The way to get the detailed effective wave function is explicitly given in the Appendix. It should be emphasized again that this treatment is just an approximation. The inaccuracy of such effective wave function is about 20% compared to the wave function obtained in the rigorous RGM calculation. This is because that due to the antisymmetrization procedure, more configurations other than $\Delta\Delta$ and C_8C_8 which span our model space are generated. Considering the uncertainty of the constituent quark model induced by the complexity of NPQCD, we believe that the contribution from those configurations is not so important. Then, our effective wave function is written as

$$\begin{aligned}|d^*(S_{d^*}=3,M_{d^*})\rangle &= [|\Delta\Delta\rangle_{S_{d^*}=3,M_{d^*}}\chi^{S,0}_{\Delta\Delta}]_{S_{d^*}=3,M_{d^*}} + [|\Delta\Delta\rangle_{S_{d^*}=3,M_S}\chi^{D,m}_{\Delta\Delta}]_{S_{d^*}=3,M_{d^*}} + [|C_8C_8\rangle_{S_{d^*}=3,M_{d^*}}\chi^{S,0}_{C_8C_8}]_{S_{d^*}=3,M_{d^*}} \\ &\quad + [|C_8C_8\rangle_{S_{d^*}=3,M_S}\chi^{D,m}_{C_8C_8}]_{S_{d^*}=3,M_{d^*}} \\ &= \sum_{ch=\Delta\Delta,C_8C_8}\sum_{pw=S,D}[|ch\rangle_{S_{d^*}=3,M_S}\chi^{pw,m_l}_{ch}(\vec{r})]_{S_{d^*}=3,M_{d^*}}\end{aligned} \tag{3}$$

with $ch = \Delta\Delta$ and C_8C_8 denoting the constituents of the component, M_{d^*} representing the magnetic quantum number of spin S_{d^*}, $pw = l = 0$ and 2 representing the S and D partial waves (pw) between the two clusters, respectively, and m_l being its magnetic quantum number. Again these four channel wave functions are orthogonal to each other. In comparison with our previous calculations for the strong decay and charge distribution where the contribution from the D-wave is ignored because it is negligibly small, here we include the relative D-wave in the calculations of the higher multipole form factors, such as $E2$, and $M3$ since those values are closely related to the matrix elements of the high-rank operators. The relative wave functions in Eq. (3), with $\chi^{S,0}_{ch}(\vec{r}) = \phi^S_{ch}(|r|)Y_{00}(\Omega_r)$ and $\chi^{D,m_l}_{ch}(\vec{r}) = \phi^D_{ch}(|r|)Y_{2m_l}(\Omega_r)$, are displayed in Fig. 1, respectively. The probabilities of S- and D-waves in the $\Delta\Delta$ and C_8C_8 channels are determined by

$$\mathcal{P}^{pw,m_l}_{ch} = \int d^3r|\chi^{pw,m_l}_{ch}(\vec{r})|^2, \tag{4}$$

and their magnitudes are shown in Table I. From Fig. 1 and Table I, one sees that comparing with corresponding D-waves, the S-wave in both $\Delta\Delta$, and C_8C_8 channels are overwhelmingly dominant, and the D-waves are negligibly small. The probability of the S-wave in the C_8C_8 channel is about 2 times larger than that in the $\Delta\Delta$ channel which is essential for our understanding of the partial widths in the double-pion and single-pion decays of d^*, and consequently of a narrow total

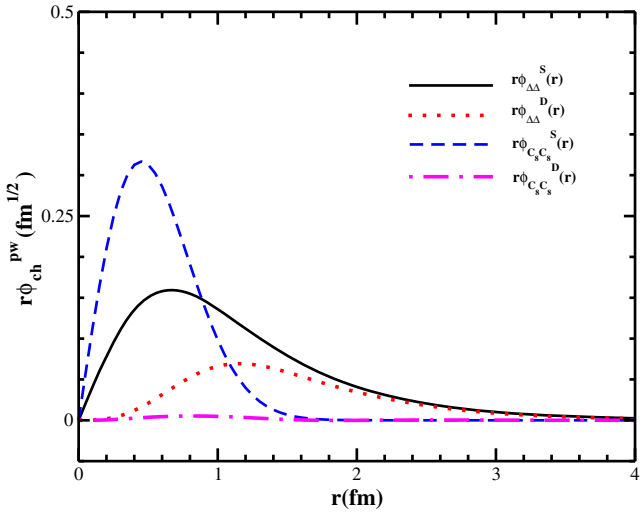

FIG. 1. Channel wave functions in the d^* system. The black solid, red dotted, blue dashed, and pink dotted-dashed curves describe the contributions from the S- and D-waves in the $\Delta\Delta$ channel, and the S- and D-waves in the C_8C_8 channel, respectively.

TABLE I. Probabilities of various components of d^*.

Channel	$\Delta\Delta$		C_8C_8	
Partial wave	S	D	S	D
Probability $\mathcal{P}_{ch}^{pw.}(\%)$	31.19	0.50	68.31	~0.002

width in our assumption of the compact structure of d^* [10–15,39].

III. MULTIPOLE DECOMPOSITION AND ELECTROMAGNETIC FORM FACTORS OF d^*

$d^*(2380)$ is a spin-3 particle, it has $2s+1=7$ form factors. In general, a traceless rank-3 tensor, $\epsilon_{\alpha\beta\gamma}$, can be employed to describe the spin-3 field. Clearly, $\epsilon_{\alpha\alpha\beta}=0$, $\epsilon_{\alpha\beta\gamma}=\epsilon_{\beta\alpha\gamma}$, and $p^\alpha\epsilon_{\alpha\beta\gamma}=0$.

In the one-photon exchange approximation, the general form of the electromagnetic current of the 3^+ particle can be written as [39]

$$\mathcal{J}^\mu=(\epsilon^*)^{\alpha'\beta'\gamma'}(p')\mathcal{M}^\mu_{\alpha'\beta'\gamma',\alpha\beta\gamma}\epsilon^{\alpha\beta\gamma}(p) \tag{5}$$

with the matrix element

$$\begin{aligned}\mathcal{M}^\mu_{\alpha'\beta'\gamma',\alpha\beta\gamma}=&[G_1(Q^2)\mathcal{P}^\mu[g_{\alpha'\alpha}(g_{\beta'\beta}g_{\gamma'\gamma}+g_{\beta'\gamma}g_{\gamma'\beta})+\text{permutations}]\\&+G_2(Q^2)\mathcal{P}^\mu[q_{\alpha'}q_\alpha[g_{\beta'\beta}g_{\gamma'\gamma}+g_{\beta'\gamma}g_{\gamma'\beta}]+\text{permutations}]/(2M_{d^*}^2)\\&+G_3(Q^2)\mathcal{P}^\mu[q_{\alpha'}q_\alpha q_{\beta'}q_\beta g_{\gamma'\gamma}+\text{permutations}]/(4M_{d^*}^4)\\&+G_4(Q^2)\mathcal{P}^\mu q_{\alpha'}q_\alpha q_{\beta'}q_\beta q_{\gamma'}q_\gamma/(8M_{d^*}^6)+G_5(Q^2)[(g^\mu_{\alpha'}q_\alpha-g^\mu_\alpha q_{\alpha'})(g_{\beta'\beta}g_{\gamma'\gamma}+g_{\beta'\gamma}g_{\beta'\gamma})+\text{permutations}]\\&+G_6(Q^2)[(g^\mu_{\alpha'}q_\alpha-g^\mu_\alpha q_{\alpha'})(q_{\beta'}q_\beta g_{\gamma'\gamma}+q_{\gamma'}q_\gamma g_{\beta'\beta}+q_{\beta'}q_\gamma g_{\gamma'\beta}+q_{\gamma'}q_\beta g_{\gamma\beta'})+\text{permutations}]/(2M_{d^*}^2)\\&+G_7(Q^2)[(g^\mu_{\alpha'}q_\alpha-g^\mu_\alpha q_{\alpha'})q_{\beta'}q_\beta q_{\gamma'}q_\gamma+\text{permutations}]/(4M_{d^*}^4)],\end{aligned} \tag{6}$$

where M_{d^*} is the mass of $d^*(2380)$, $\mathcal{P}=p'+p$ (with p' and p being the momenta of the outgoing and incoming d^*, respectively), and $G_i(Q^2)$, $i=1,2,\ldots,7$, are the seven electromagnetic form factors which depend on the momentum transfer square $Q^2=|\vec{q}|^2$. The gauge invariant condition

$$q_\mu\mathcal{M}^\mu_{\alpha'\beta'\gamma',\alpha\beta\gamma}=0 \tag{7}$$

should also be fulfilled, as well as the time-reversal invariance. In general, the physical form factors, such as the charge monopole $C0$, electric quadrupole $E2$, hexadecapole $C4$, and tetrahexacontapole $C6$ form factors, as well as the magnetic dipole $M1$, octupole $M3$ and dotriacontapole $M5$ form factors, can be constructed by the combinations of the seven electromagnetic form factors $G_i(Q^2)$, $i=1,2,\ldots7$.

The multipole decompositions of the electromagnetic currents, as well as the electromagnetic form factors of a particle with spin-2 or with arbitrary spin, have been explicitly discussed in Refs. [56–59]. According to those analysis, in the quark degrees of freedom, the time component of the photon-d^* electromagnetic current, in the instantaneous approximation, is $J^0=\sum_{i=1}^6 j_i^0$ with j_i^0 denoting the time component of the photon-quark electromagnetic current for the i-th quark. The electric charge lth multipole form factor of d^* reads

$$G_l^E(Q^2)=\frac{(2M_{d^*})^l}{e}\sqrt{\frac{4\pi}{2l+1}}\frac{(2l+1)!!}{l!Q^l}\mathcal{I}_{El}(Q^2), \tag{8}$$

with e being the unit of charge and

$$\begin{aligned}\mathcal{I}_{El}(Q^2)=&\langle d^*|\sum_{i=1}^6\int d^3r[d^3X]e_ij_l(Q|\vec{r}_i-\vec{R}|)Y_{l0}(\Omega_{r_i})|d^*\rangle\\=&3\langle d^*|\int d^3r[d^3X][e_3j_l(Q|\vec{r}_3-\vec{R}|)Y_{l0}(\Omega_{\vec{r}_3-\vec{R}})\\&+e_6j_l(Q|\vec{r}_6-\vec{R}|)Y_{l0}(\Omega_{\vec{r}_6-\vec{R}})]|d^*\rangle,\end{aligned} \tag{9}$$

where $[d^3X] = d^3\rho_1 d^3\rho_2 d^3\lambda_1 d^3\lambda_2$, ρ_1, ρ_2, λ_1, and λ_2 are the conventional Jacobi variables in the two clusters, and j_l represents the lth spherical Bessel function.

The multipole decomposition of the space component of the electromagnetic current in the momentum space gives [58,59]

$$\langle d^*|\rho^M(\vec{q})|d^*\rangle = e\sum_{l=0}^{+\infty} i^l \tau^{l/2} \frac{l+1}{\tilde{C}^{l-1}_{2l-1}} G_{Ml}(Q^2) Y_{l0}(\Omega_q), \quad (10)$$

where $\rho^M(\vec{q})$ denotes the magnetic density of the system with $\tau = \frac{Q^2}{4M^2_{d^*}}$, and

$$\tilde{C}^k_n = \begin{cases} \frac{n!!}{k!!(n-k)!!}, & n \geq k \geq -1, \\ 0, & \text{otherwise.} \end{cases} \quad (11)$$

If we only consider the quark-photon coupling, we can write the magnetic density as $\rho^M(\vec{r}) = \sum_{i=1}^6 \vec{\nabla}\cdot(\vec{j}_i(r)\times\vec{r}_i)$ with $\vec{j}_i(r)$ and $\vec{r}_i$ being the current and position vectors for the ith quark in the coordinate space, and $\rho^M(\vec{q}) = \sum_{i=1}^6 \vec{\nabla}\cdot[(e_i\vec{\sigma}_i\times\vec{q})\times\vec{q}] = 2\sum_{i=1}^6 e_i\vec{\sigma}_i\cdot\vec{q}$ with $\vec{\sigma}_i$, e_i, and $\vec{q}$ being the Pauli matrix, the charge for the ith quark and the transferred momentum, respectively. Then, we have

$$\begin{aligned}\langle d^*|\rho^M(\vec{q})|d^*\rangle &= \sum_{i=1}^6 \langle d^*|\rho^M_i(\vec{q})|d^*\rangle \\ &= \frac{6i}{2m_q}\langle d^*|[e_3\vec{\sigma}_3\cdot\vec{q} + e_6\vec{\sigma}_6\cdot\vec{q}]|d^*\rangle. \end{aligned} \quad (12)$$

By assuming that the form factors are the functions of the momentum transfer square Q^2 in the one-photon exchange approximation, we have [58,59]

$$\begin{aligned} G_{M1}(Q^2) = &-\int d\Omega_q Y^*_{10}(\Omega_q)\frac{1}{2}\frac{i}{e\sqrt{\tau(Q)}} \\ &\times\sqrt{\frac{3}{4\pi}}\langle d^*|\rho^M(\vec{q})|d^*\rangle, \end{aligned} \quad (13)$$

for $M1$ and

$$\begin{aligned} G_{M3}(Q^2) = &+\int d\Omega_q Y^*_{30}(\Omega_q)\frac{i}{2e\tau(Q)\sqrt{\tau(Q)}} \\ &\times\sqrt{\frac{7}{4\pi}}\frac{5}{4}\langle d^*|\rho^M(\vec{q})|d^*\rangle, \end{aligned} \quad (14)$$

for $M3$, respectively.

IV. NUMERICAL RESULTS AND DISCUSSIONS

By using the wave functions of d^* in Eq. (3), the charge monopole $C0$, electric quadrupole $C2$, magnetic dipole $M1$, and magnetic octupole $M3$ form factors for d^* are calculated. It should be mentioned that since the charge monopole form factor (or the charge distribution) of d^* has already been discussed explicitly in our previous paper [39], we do not reiterate the relevant result in detail in this work. It is shown that the charge distribution receives the dominant contribution from the S partial wave, namely the $S-S$ matrix elements of the $\Delta\Delta$ and C_8C_8 components. Based on the fact that the slope of the charge distribution is related to the root-mean-square radius (rms) of the d^* system, it is found that compared to the $D_{12}\pi$ (or $\Delta\pi N$) structure, as well as to a single $\Delta\Delta$ structure, a compact hexaquark dominated structure for d^*, which is deduced from our coupled $\Delta\Delta + C_8C_8$ channel RGM calculation, has a much smaller rms [39].

The magnetic dipole form factor $G_{M1}(Q^2)$ of d^* is plotted in Fig. 2. This form factor respectively receives the contributions from the $S-S$ matrix elements of the $\Delta\Delta$ and C_8C_8 components, which are described by the blue-dashed and red-dotted curves in Fig. 2. Other contributions from the $S-D$ matrix element (the off-diagonal matrix element between the S-wave and D-wave functions) and the $D-D$ matrix element (the diagonal matrix element between D-wave functions) are negligibly small compared to the $S-S$ components. These features can also be corroborated by the purple-dotted-dashed and pink-double-dotted-dashed curves in Fig. 2. Clearly, the major contribution cames from the S-wave of the C_8C_8 component, however the contribution from the S-wave of the $\Delta\Delta$ component is also sizable. This is because that the probability of the C_8C_8 component is almost twice of that of the $\Delta\Delta$ component.

For a comparison, the calculated magnetic dipole form factor of d^* with a single channel $\Delta\Delta$ structure is demonstrated by the green double-dashed-dotted curve also in Fig. 2. Furthermore, the magnetic dipole momentum of d^*, μ_{d^*}, can be extracted from the magnetic dipole form factor at zero momentum transfer $G_{M1}(Q^2=0)$. The

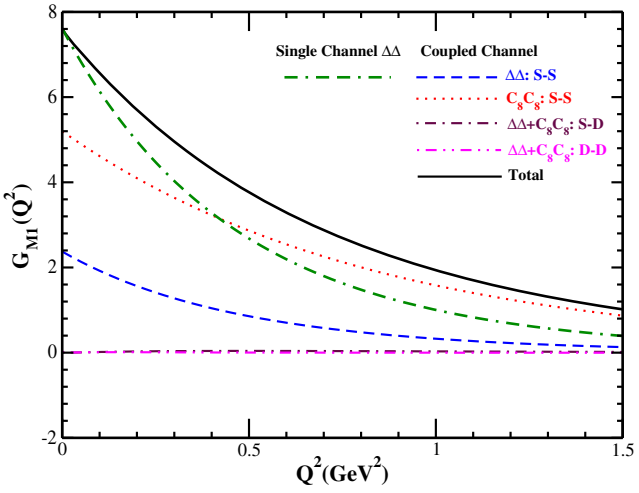

FIG. 2. The magnetic dipole form factor $M1$ of d^*.

obtained magnetic dipole moment of d^* in the coupled channel $\Delta\Delta + C_8C_8$ cases is about 7.602 in unit of e. Comparing with the proton and neutron magnetic dipole moments of 2.79 and -1.91, respectively, this value is understandable, because the number of quarks in d^* is twice of that in the proton or neutron. Moreover, the calculated magnetic dipole moment of d^* with a single $\Delta\Delta$ structure is about 7.612 which is almost the same as that of the d^* state with a $\Delta\Delta + C_8C_8$ structure. The tiny difference between two magnetic dipole moments with different structures may be due to the different amount of D-wave contributions. In addition, it should be particularly stressed that the contribution from the off-diagonal matrix element between the $\Delta\Delta$ and C_8C_8 channels vanishes since the former has two colorless clusters and the latter has two colored clusters, and the electromagnetic interaction is color-independent.

In the naive constituent quark model (NCQM), it is known that the magnetic moments of the proton and neutron are about $M_N/m_q \sim 3$ and $-2M_N/3m_q \sim -2$, respectively. These values roughly agree with the experimental data of 2.79 and -1.91. In the d^* case, we find that, in the naive quark model, the contributions from the $\Delta\Delta$ and C_8C_8 components are all proportional to M_{d^*}/m_q due to $I(J^P) = 0(3^+)$ for d^* and the quantum numbers of the Δ and C_8 clusters. Consequently, the magnetic moment of d^*, which relates to its magnetic form factor at the real photon limit, is

$$G_{M1}^{NCQM}(0) = [\mathcal{P}^S_{\Delta\Delta} + \mathcal{P}^S_{C_8C_8}]\frac{3M_{d^*}}{M_N} \sim \frac{3M_{d^*}}{M_N} = 7.62, \quad (15)$$

where we approximately take $[\mathcal{P}^S_{\Delta\Delta} + \mathcal{P}^S_{C_8C_8}] \sim 1$ for the S-wave as shown in Table I, and $m_q \sim M_N/3$. This magnetic moment is very close to the calculated value of 7.602 obtained from $G_{M1}(0)$ mentioned above. From the results for the proton, neutron and d^*, one may believe that the magnetic moment of a particle estimated in the naive constituent quark model can be taken as a qualitative reference in the study of the hadronic magnetic moment. The absolute ratio of the calculated magnetic moment of the $\Delta\Delta$ component to that of the C_8C_8 component in our approach is

$$R^{\Delta\Delta}_{C_8C_8} = \frac{G^{\Delta\Delta}_{M1}}{G^{C_8C_8}_{M1}} = \frac{2.37}{5.20} = 0.4558, \quad (16)$$

which is almost the same as the probability ratio of the two component $\mathcal{P}^S_{\Delta\Delta}/\mathcal{P}^S_{C_8C_8} = 31.19\%/68.31\% = 0.4566$ shown in Table I. Moreover, in the naive constituent quark model, by using the same method, we obtain the magnetic moment of the d^* state with a single $\Delta\Delta$ structure as

$$\tilde{\mu}^{\Delta\Delta}_{d^*} = \tilde{G}^{\Delta\Delta}_{M1}(0) \sim \frac{3M_{d^*}}{M_N} = 7.62. \quad (17)$$

This value is the same as that with a compact hexaquark dominated structure, which is understandable because the averaged magnetic moment in the $\Delta\Delta$ component is the same as that in the C_8C_8 component.

In addition, the magnetic moment of d^* with a $D_{12}\pi$ interpretation can also be calculated in this way. We know that the spin of pion is zero, the contribution from the orbital angular moment between the D_{12} and π systems vanishes. Then, the magnetic moment of d^* comes from the D_{12} cluster only. Therefore, the obtained magnetic moment of d^* in the naive constituent quark model is

$$\mu^{D_{12}\pi}_{d^*} = G^{D_{12}\pi}_{M1,d^*}(0) \sim \frac{2M_{d^*}}{M_N} = 5.07. \quad (18)$$

From the above obtained values for the different inner structures of d^*, one sees that the magnetic moment can also serve as a quantity to distinguish between the compact hexaquark dominated structure (or the $\Delta\Delta$ structure) and the $D_{12}\pi$ structure, but not between the $\Delta\Delta + C_8C_8$ compact hexaquark dominated structure and the $\Delta\Delta$ structure.

Furthermore, we know that the slope of G_{M1} is related to the magnetic radius of d^*. To see the different contributions to the magnetic radius from the $\Delta\Delta$ component and the C_8C_8 component, we check the slopes of $G^{\Delta\Delta}_{M1}(Q^2)$ and $G^{C_8C_8}_{M1}(Q^2)$. They are

$$\begin{aligned} -\frac{d}{dQ^2}G^{\Delta\Delta}_{M1}(Q^2)\Big|_{Q^2\to 0} &= 5.014\,\mathrm{GeV}^{-2} = 0.195\,\mathrm{fm}^2, \\ -\frac{d}{dQ^2}G^{C_8C_8}_{M1}(Q^2)\Big|_{Q^2\to 0} &= 6.139\,\mathrm{GeV}^{-2} = 0.239\,\mathrm{fm}^2, \end{aligned} \quad (19)$$

and their ratio is

$$R = \frac{\frac{d}{dQ^2}G^{\Delta\Delta}_{M1}(Q^2)|_{Q^2\to 0}}{\frac{d}{dQ^2}G^{C_8C_8}_{M1}(Q^2)|_{Q^2\to 0}} \sim 0.816. \quad (20)$$

This ratio contains the contributions from $\mathcal{P}^S_{\Delta\Delta}$ and $\mathcal{P}^S_{C_8C_8}$, as well as from the Q^2 dependent wave functions of the $\Delta\Delta$ and C_8C_8 components. The obtained value is remarkably different with the probability ratio $R^{\Delta\Delta}_{C_8C_8} \sim 0.4558$, which reveals a fact that although the probability of the $\Delta\Delta$ component is much smaller than that of the C_8C_8 component, but the normalized magnetic radius of the $\Delta\Delta$ component is larger than that of the C_8C_8 component, namely comparing with the C_8C_8 component, the wave function of the $\Delta\Delta$ component distributes in a wider range. As a final result, when d^* has a compact hexaquark

dominant structure, the obtained slope of the magnetic form factor G_{M1} at the zero momentum transfer is

$$-\frac{d}{dQ^2}G_{M1}(Q^2)\Big|_{Q^2\to 0} = 0.434\ \text{fm}^2, \tag{21}$$

and corresponding magnetic radius is

$$\left[\left|-\frac{d}{dQ^2}G_{M1}(Q^2)\Big|_{Q^2\to 0}\right|\right]^{1/2} = 0.659\ \text{fm}. \tag{22}$$

In addition, in the single channel $\Delta\Delta$ case, we have the magnetic radius being

$$\left[\left|-\frac{d}{dQ^2}G^S_{M1}(Q^2)\Big|_{Q^2\to 0}\right|\right]^{1/2} = 0.896\ \text{fm}. \tag{23}$$

Clearly, one sees that the magnetic radius of d^* with a single $\Delta\Delta$ structure is apparently larger than that with a compact hexaquark dominated structure. Therefore, we believe that the magnetic radius of d^* can serve as a physical quantity to distinguish between the $\Delta\Delta + C_8C_8$ and $\Delta\Delta$ structures of d^*. Moreover, we stress that the magnetic feature of d^* is consistent to the phenomenon revealed in the case of the charge distribution of d^*, and the charge radius of d^* [39] is slightly larger than its magnetic radius. These characters also appeared in the experimental measurements for deuteron as has been discussed in Ref. [60].

Our calculated electric quadrupole form factor G_{E2} is shown in Fig. 3. In this figure, the blue-dashed and red-dotted, purple-dotted-dashed, and pink-double-dotted-dashed curves describe the contributions from the matrix elements between the S- and D-waves and the D- and D-waves of the $\Delta\Delta$ component and from the matrix elements between the S- and D-waves and the D- and D-waves of the C_8C_8 component, respectively. It should be mentioned that in this rank-2 operator case, the diagonal matrix element between S-waves ($S-S$) does not contribute. The dominant contribution to G_{E2} comes from the off-diagonal matrix element between the S- and D-waves ($S-D$ or $D-S$) of the $\Delta\Delta$ component. Since the probability of the D-wave of the C_8C_8 component is much smaller than that of the $\Delta\Delta$ component as shown in Table I, the contribution from the D-wave of the C_8C_8 component is negligibly small. Moreover, we have $G_{E2}(0) = \frac{M^2_{d^*}}{e}Q^{d^*}_{20}$, where $Q^{d^*}_{20}$ denotes the quadrupole deformation of d^*. Our calculation shows that such a deformation is about $Q^{d^*}_{20} = 2.53\times 10^{-2}$ fm^2, which is much smaller than that of the deuteron $Q^d_{20} = 0.259$ fm^2. This is because that the dominant contribution for the electric quadrupole moment comes from the $S-D$ matrix element of the colorless-cluster component, namely the $\Delta\Delta$ component in d^*, as well as from that of the $p-n$ component in the deuteron case, however, the probability of the $\Delta\Delta$ component in d^* is only about $1/3$ and the probability of the $p-n$ component in deuteron is almost 1, meanwhile the probability of the D-wave in the $\Delta\Delta$ component of d^* (about 0.5%) is much smaller than that in the $p-n$ component of deuteron (about 5%). These quadrupole deformations also indicate that d^* is more inclined to a slightly oblate shape. Therefore, our d^* looks a more compact and spherical-shape due to its wave function.

It is known that the deformations of the nucleon and Δ give the $E2/M1$ ratio for the $\gamma N\to\Delta$ transition amplitude, which is one of the significant observables for judging different models. Here, one can also consider the deformation in the Δ wave function. According to the previous analysis (see for example Refs. [61–63]), the mixing coefficient for the component $\Delta^4D_s(\frac{3}{2})^+$ in the Δ resonance is about -0.11, the probability of such a configuration is about 1.2%, and the obtained $E2/M1\simeq -1.0\%$ for the ΔN transition. We can check the effect of the deformation of Δ

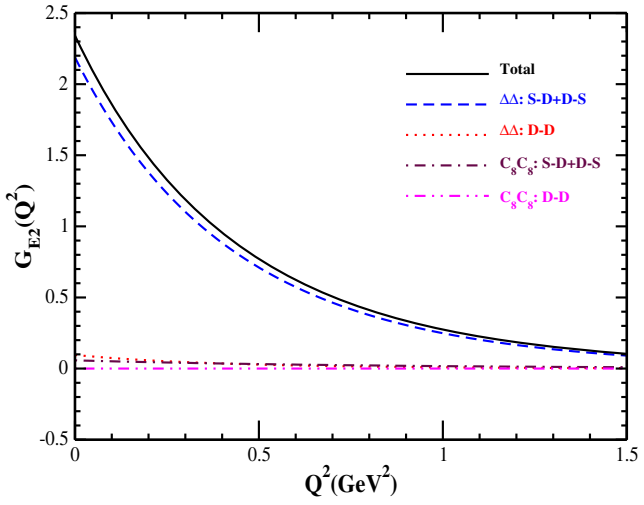

FIG. 3. The quadrupole form factor of d^*.

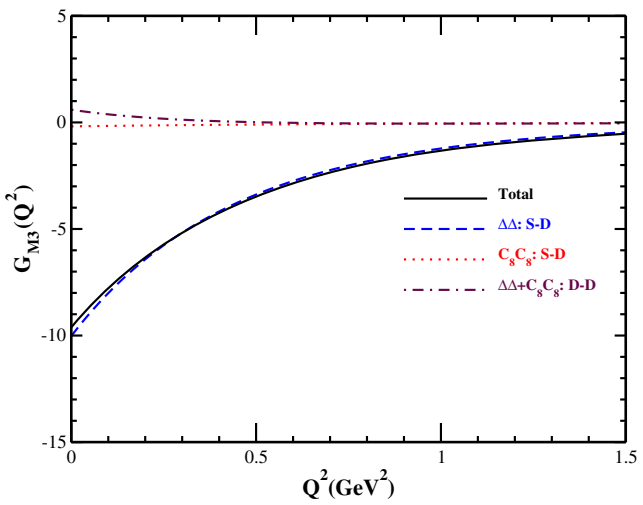

FIG. 4. The magnetic octupole $M3$ form factor of d^*.

on the quadrupole moment. Our numerical calculation shows that this effect provides a suppression of about 0.25% to the quadrupole moment of d^*.

Finally, we also shown the magnetic octupole form factor of d^* in Fig. 4, where the blue-dashed, red-dotted, and purple-dotted-dashed curves represent the contributions from the matrix elements between the S- and D-waves of the $\Delta\Delta$ and C_8C_8 components and between the D-waves of the whole $\Delta\Delta + C_8C_8$ wave function. Still, the major contribution comes from the $S-D$ matrix element of the $\Delta\Delta$ component as well.

V. SUMMARY

In order to understand the internal structure of the d^* resonance discovered by CELSIUS/WASA and WASA@COSY Collaborations, two major structural schemes were proposed recently. One of them considers that it has a compact exotic hexaquark dominated structure and the other proposal believes that it is basically a molecular-like hadronic state. These two structure models have been tested in terms of the experimental data. Up to now, both models can explain the mass, the total width, and the partial decay widths for all the observed double pion decays of the d^* resonance. However, for a single pion decay process, although the observed upper limit of the branching ratio can be explained by both structure models, the ways of explanation have a subtle difference. The result from a compact hexaquark dominated structure model is directly calculated and is consistent with the data. On the other side, a combined $\alpha[\Delta\Delta] + (1-\alpha)[D_{12}\pi]$ mixing structure was also proposed [17], and the data can be explained as well. Therefore, we need to seek other observable physical quantities to distinguish these two different structures for d^*.

Here, based on the studies on the electromagnetic form factors for the nucleon, deuteron, and even vector mesons, we propose that the electromagnetic form factors, including the d^* charge distribution in our former paper [39], can be the desirable physical quantities for distinguishing different structure approaches. In this paper, we study the $M1$, $E2$, and $M3$ form factors in addition to the former reported charge form factor $C0$ by employing the wave functions obtained in the coupled $\Delta\Delta + C_8C_8$ channel RGM calculation based on our chiral constituent quark model. It is found that in the case with a compact $\Delta\Delta + C_8C_8$ structure, since the D-wave components in both $\Delta\Delta$ and C_8C_8 channels are negligible small, less than 0.5% of the total wave function, its contribution to the electromagnetic form factor $M1$ is rather small in comparison with that from the S-wave component. However, for the electromagnetic form factors $E2$ and $M3$, the contribution of the D-wave associating with the S-wave, namely the off-diagonal matrix elements between the D- and S-waves, of the $\Delta\Delta$ component dominates. The extracted magnetic dipole moments of d^* for the compact hexaquark dominated ($\Delta\Delta + C_8C_8$) structure, the pure $\Delta\Delta$ structure, and the $D_{12}\pi$ structure are 7.602, 7.612, and 5.07, respectively. The corresponding magnetic radii are about 0.66 fm in the case with a coupled $\Delta\Delta + C_8C_8$ structure and about 0.90 fm in the case with a single $\Delta\Delta$ structure, respectively. These results indicate that the magnetic moment can be used to distinguish between the compact hexaquark dominated structure (or the pure $\Delta\Delta$ structure) and the $D_{12}\pi$ structure, but not between the compact hexaquark dominated structure and the pure $\Delta\Delta$ structure. However, the magnetic radius can be considered as a physical quantity to discriminate the $\Delta\Delta + C_8C_8$ and $\Delta\Delta$ structures. Moreover, a quite small quadrupole deformation $\hat{Q}^{d^*}_{20}$ of 2.53×10^{-2} fm^2 for the d^* state with a $\Delta\Delta + C_8C_8$ structure indicates that, differing with deuteron, d^* is more inclined to a slightly oblate shape, and consequently, a compact hexaquark dominated and spherical structure. The effect of the deformation of the Δ resonance provides a suppression of about 0.25% to the quadrupole moment of d^*.

Combining the results for $C0$ in our previous paper [39], we come to the conclusion that the charge radius and magnetic moment of d^* can be used as new physical quantities to discriminate among different structure models. It is expected that these theoretically predicted quantities, especially in the low-Q region, can be measured by experiments in the near future. For instance [64], at Belle II, with its high luminosity, it might be possible to access $e^+ + e^- \to d^* + \bar{d}^*$, and then one might extract some information about the electromagnetic form factors of d^* in the time-like region. Considering the photo-production process, one might access magnetic moment information by photo-exciting the P-shell nucleon pair with the M1 transition as well. There is another possible chance to directly access the information of the electromagnetic feature of d^* at the low-Q region, where one may look for a e^+e^- pair production process ($pn \to d^*e^+e^-$) at the WASA@GSI and CBM due to the advantages of their deuteron beam and a very good di-lepton efficiency and triggering in the CBM experiment.

ACKNOWLEDGMENTS

This work is supported by the National Natural Science Foundations of China (NSFC) under the Grants No. 11475192, No. 11521505, and No. 11565007, the Sino-German CRC 110 "Symmetries and the Emergence of Structure in QCD" project by NSFC under the Grant No. 11621131001, the Key Research Program of Frontier Sciences, Chinese Academy of Sciences, Grant No. Y7292610K1, and the IHEP Innovation Fund under the Grant No. Y4545190Y2. Authors thank the fruitful discussions with Mikhail Bashkanov and Y. D. thanks Fei Huang for providing the wave functions of d*.

APPENDIX: d^* IN CHIRAL CONSTITUENT QUARK MODEL

The six-quark system with $[I(J^P) = 0(3^+)]$, named d^*, is studied in the quark degrees of freedom by employing the

chiral SU(3) constituent quark model [40,41]. In this model, the interactive Lagrangian between quark and scaler and pseudoscalar chiral fields is written as

$$\mathcal{L}_I^{\rm ch} = -g_{\rm ch}\bar{\psi}\left(\sum_{a=0}^{8}\lambda_a\sigma_a + i\gamma_5\sum_{a=0}^{8}\lambda_a\pi_a\right)\psi, \quad \text{(A1)}$$

and the interactive Lagrangian between quark and vector meson fields as

$$\mathcal{L}_I^{\rm chv} = -g_{\rm chv}\bar{\psi}\gamma_\mu\lambda_a\rho_a^\mu\psi - \frac{f_{\rm chv}}{2M_N}\bar{\psi}\sigma_{\mu\nu}\lambda_a\partial^\mu\rho_a^\nu\psi. \quad \text{(A2)}$$

Then the total Hamiltonian of the system can be formulated as

$$H = \sum_{i=1}^{6}T_i - T_G + \sum_{j>i=1}^{6}(V_{ij}^{\rm OGE} + V_{ij}^{\rm conf} + V_{ij}^{\rm ch} + V_{ij}^{\rm chv}), \quad \text{(A3)}$$

with $V_{ij}^{\rm ch}$ and $V_{ij}^{\rm chv}$ being the chiral field and vector meson field induced effective interactions, respectively, between the ith quark and the jth quark,

$$V_{ij}^{\rm ch} = \sum_{a=0}^{8}V_{ij}^{\sigma_a} + \sum_{a=0}^{8}V_{ij}^{\pi_a}, \quad \text{(A4)}$$

and

$$V_{ij}^{\rm chv} = \sum_{a=0}^{8}V_{ij}^{\rho_a}, \quad \text{(A5)}$$

where V^{σ_a}, V^{π_a}, and V^{ρ_a} are the potentials induced by the scalar, pseudoscalar and vector meson fields, respectively, T_i the kinetic energy operator for the ith quark, T_G the kinetic energy operator for the center of mass motion of the system, $V^{\rm OGE}$ and $V^{\rm conf}$ the one-gluon-exchange and confinement potentials, respectively. The model with vector meson induced potentials is later renamed as the extended chiral SU(3) constituent quark model. The parameters of the model are determined by fitting the experimental data of the masses of the ground state baryons, the phase shifts and cross sections of the NN scattering, the binding energy of deuteron, etc. The detailed forms of the potentials, model parameter determinations and resultant values of parameters can be found in Refs. [41,42].

To investigate the properties of this six quark system microscopically, one usually use a so-called resonating group method (RGM). In this framework, we proposed a trial wave function in the form of

$$\Psi_{6q} = \mathcal{A}\Big[\hat{\phi}_\Delta^A(\vec{\xi}_1,\vec{\xi}_2,\mu_\Delta^A)\hat{\phi}_\Delta^B(\vec{\xi}_4,\vec{\xi}_5,\mu_\Delta^B)\eta_{\Delta\Delta}(\vec{r}) + \hat{\phi}_{\rm C_8}^A(\vec{\xi}_1,\vec{\xi}_2,\mu_{\rm C_8}^A)\hat{\phi}_{\rm C_8}^B(\vec{\xi}_4,\vec{\xi}_5,\mu_{\rm C_8}^B)\eta_{\rm C_8C_8}(\vec{r})\Big]_{S=3,T=0}^{C=(00)},$$

where S, T, and C represent the quantum numbers of the spin, isospin, and color, $\mathcal{A} = 1 - \sum_{i(\in A),j(\in B)}P_{ij}^{OSFC}$ is the total antisymmetrization operator, P_{ij}^{OSFC} denotes the exchange operator which exchanges the ith quark belonging to the cluster A and jth quark pertaining to the cluster B in the orbital, spin, flavor, and color spaces, $\hat{\phi}_{\Delta(\rm C_8)}^{A(B)}$ is the antisymmetrized internal wave function of the (1,2,3) ((4,5,6)) quark cluster A(B) for either Δ or C_8 with $\vec{\xi}_i$ ($i = 1, 2(4,5)$) being its internal Jacobi coordinates and $\mu_{\Delta(\rm C_8)}^{A(B)}$ being an aggregate of the quantum numbers of the spin, isospin, and color of the $\Delta(\rm C_8)$ cluster named A(B) with $[S,I,C]_{\Delta(\rm C_8)} = [3/2,3/2,(00)((3/2,1/2,(11)))]$ for the $\Delta(\rm C_8)$ cluster, $\eta_{\Delta\Delta(\rm C_8C_8)}$ is the relative wave function between A and B clusters which will be determined by the dynamical calculation of the system with the (extended) chiral SU(3) constituent quark model.

The binding energy relative to the threshold of the $\Delta\Delta$ channel and corresponding relative wave functions between clusters are obtained by numerically solving the bound state RGM equation [10,11]

$$\langle\delta\Psi_{6q}|H - E|\Psi_{6q}\rangle = 0.$$

This is a standard treatment in few-body physics. There are many studies about baryon-baryon interactions carried out by using this RGM method [8,41,45–52].

It should be mentioned that due to the nonorthogonality of the base functions used in the dynamical calculation, the two components in Eq. (1) are not orthogonal to each other. Therefore, the wave function in the current form is not suitable for the ongoing study.

On the other hand, in terms of $\mathcal{A}$, Eq. (1) can be rewritten as

$$\begin{aligned}\Psi_{6q} = {} & \Big[\hat{\phi}_\Delta(\vec{\xi}_1,\vec{\xi}_2,\mu_\Delta^A)\hat{\phi}_\Delta(\vec{\xi}_4,\vec{\xi}_5,\mu_\Delta^B)\eta_{\Delta\Delta}(\vec{r})\Big]_{S=3,T=0}^{C=(00)} + \Big[\hat{\phi}_{\rm C_8}(\vec{\xi}_1,\vec{\xi}_2,\mu_{\rm C_8}^A)\hat{\phi}_{\rm C_8}(\vec{\xi}_4,\vec{\xi}_5,\mu_{\rm C_8}^B)\eta_{\rm C_8C_8}(\vec{r})\Big]_{S=3,T=0}^{C=(00)} \\ & - \sum_{i(\in A),j(\in B)}P_{ij}^{OSFC}\Big[\hat{\phi}_\Delta(\vec{\xi}_1,\vec{\xi}_2,\mu_\Delta^A)\hat{\phi}_\Delta(\vec{\xi}_4,\vec{\xi}_5,\mu_\Delta^B)\eta_{\Delta\Delta}(\vec{r})\Big]_{S=3,T=0}^{C=(00)} \\ & - \sum_{i(\in A),j(\in B)}P_{ij}^{OSFC}\Big[\hat{\phi}_{\rm C_8}(\vec{\xi}_1,\vec{\xi}_2,\mu_{\rm C_8}^A)\hat{\phi}_{\rm C_8}(\vec{\xi}_4,\vec{\xi}_5,\mu_{\rm C_8}^B)\eta_{\rm C_8C_8}(\vec{r})\Big]_{S=3,T=0}^{C=(00)}, \quad \text{(A6)}\end{aligned}$$

where, on the right-hand side, the first 2 terms are direct terms and the latter 2 terms are exchange terms. It is clear that the direct terms have a quite simple form, but the exchange terms are very complicated due to intricate exchange operations. In order to make the wave functions of different channels orthogonal to each other, to make the numerical calculations simplified and feasible, and not to miss the important effect of the antisymmetrization, it is better to express the wave function approximately in a form without the exchange operator phenomenologically, namely a form of the direct term, but still keep the effect of the totally antisymmetrized feature of the wave function of the system

$$\Psi_{6q}^{\rm eff}=\hat{\phi}_{\Delta}^{A}(\vec{\xi}_1,\vec{\xi}_2,\mu_{\Delta}^{A})\hat{\phi}_{\Delta}^{B}(\vec{\xi}_4,\vec{\xi}_5,\mu_{\Delta}^{B})\chi_{\Delta\Delta}(\vec{r})+\hat{\phi}_{\rm C_8}^{A}(\vec{\xi}_1,\vec{\xi}_2,\mu_{\rm C_8}^{A})\hat{\phi}_{\rm C_8}^{B}(\vec{\xi}_4,\vec{\xi}_5,\mu_{\rm C_8}^{B})\chi_{\rm C_8C_8}(\vec{r}). \tag{A7}$$

One of the ways to realize it is carrying out a so-called projection procedure. For instance, to obtain an effective relative wave function $\chi_{\Delta\Delta}(\vec{r})$ between two Δ clusters in the $\Delta\Delta$ component of the approximated effective wave function in the above mentioned simpler form like the direct term, $[\hat{\phi}_{\Delta}(\vec{\xi}_1,\vec{\xi}_2,\mu_{\Delta}^{A})\hat{\phi}_{\Delta}(\vec{\xi}_4,\vec{\xi}_5,\mu_{\Delta}^{B})\chi_{\Delta\Delta}(\vec{r})]$, what one should do is multiplying Eq. (A6) by $\hat{\phi}_{\Delta}^{*}(\vec{\xi}_1,\vec{\xi}_2,\mu_{\Delta}^{A})\hat{\phi}_{\Delta}^{*}(\vec{\xi}_4,\vec{\xi}_5,\mu_{\Delta}^{B})$ and integrating over all internal Jacobi coordinates $\vec{\xi}_i$ $(i=1,2,4,5)$

$$\begin{aligned}\chi_{\Delta\Delta}(\vec{r})&=\langle\phi_{\Delta}(\vec{\xi}_1,\vec{\xi}_2,\mu_{\Delta}^{A})\phi_{\Delta}(\vec{\xi}_4,\vec{\xi}_5,\mu_{\Delta}^{B})|\Psi_{6q}\rangle\\&=\eta_{\Delta\Delta}(\vec{r})-\left\langle\hat{\phi}_{\Delta}(\vec{\xi}_1,\vec{\xi}_2,\mu_{\Delta}^{A})\hat{\phi}_{\Delta}(\vec{\xi}_4,\vec{\xi}_5,\mu_{\Delta}^{B})\Big|\sum_{i(\in A),j(\in B)}P_{ij}^{OSFC}[\hat{\phi}_{\Delta}(\vec{\xi}_1,\vec{\xi}_2,\mu_{\Delta}^{A})\hat{\phi}_{\Delta}(\vec{\xi}_4,\vec{\xi}_5,\mu_{\Delta}^{B})\eta_{\Delta\Delta}(\vec{r})]\right\rangle\\&\quad-\left\langle\hat{\phi}_{\Delta}(\vec{\xi}_1,\vec{\xi}_2,\mu_{\Delta}^{A})\hat{\phi}_{\Delta}(\vec{\xi}_4,\vec{\xi}_5,\mu_{\Delta}^{B})\Big|\sum_{i(\in A),j(\in B)}P_{ij}^{OSFC}[\hat{\phi}_{\rm C_8}(\vec{\xi}_1,\vec{\xi}_2,\mu_{\rm C_8}^{A})\hat{\phi}_{\rm C_8}(\vec{\xi}_4,\vec{\xi}_5,\mu_{\rm C_8}^{B})\eta_{\rm C_8C_8}(\vec{r})]\right\rangle\end{aligned}$$

This effective relative wave function consists of three terms. The first term is the original relative wave function in the $\Delta\Delta$ component obtained by the dynamical calculation. The second one describes the effect of antisymmetrization (or exchanges) in the $\Delta\Delta$ component. The third one denotes the contribution of the antisymmetrization (or exchange) effect from the $\rm C_8C_8$ component. Clearly, this effective relative wave function includes almost all the anti-symmetrization effect of the $\Delta\Delta$ component in Eq. (1). Similarly, we can get the effective relative wave function for the $\rm C_8C_8$ component as

$$\begin{aligned}\chi_{\rm C_8C_8}(\vec{r})&=\langle\phi_{\rm C_8}(\vec{\xi}_1,\vec{\xi}_2,\mu_{\rm C_8}^{A})\phi_{\rm C_8}(\vec{\xi}_4,\vec{\xi}_5,\mu_{\rm C_8}^{B})|\Psi_{6q}\rangle\\&=\eta_{\rm C_8C_8}(\vec{r})-\left\langle\hat{\phi}_{\rm C_8}(\vec{\xi}_1,\vec{\xi}_2,\mu_{\rm C_8}^{A})\hat{\phi}_{\rm C_8}(\vec{\xi}_4,\vec{\xi}_5,\mu_{\rm C_8}^{B})\Big|\sum_{i(\in A),j(\in B)}P_{ij}^{OSFC}[\hat{\phi}_{\rm C_8}(\vec{\xi}_1,\vec{\xi}_2,\mu_{\rm C_8}^{A})\hat{\phi}_{\rm C_8}(\vec{\xi}_4,\vec{\xi}_5,\mu_{\rm C_8}^{B})\eta_{\rm C_8C_8}(\vec{r})]\right\rangle\\&\quad-\left\langle\hat{\phi}_{\rm C_8}(\vec{\xi}_1,\vec{\xi}_2,\mu_{\rm C_8}^{A})\hat{\phi}_{\rm C_8}(\vec{\xi}_4,\vec{\xi}_5,\mu_{\rm C_8}^{B})\Big|\sum_{i(\in A),j(\in B)}P_{ij}^{OSFC}[\hat{\phi}_{\Delta}(\vec{\xi}_1,\vec{\xi}_2,\mu_{\Delta}^{A})\hat{\phi}_{\Delta}(\vec{\xi}_4,\vec{\xi}_5,\mu_{\Delta}^{B})\eta_{\Delta\Delta}(\vec{r})]\right\rangle\end{aligned}$$

Due to the orthogonality of $[\hat{\phi}_{\Delta}(\vec{\xi}_1,\vec{\xi}_2,\mu_{\Delta}^{A})\hat{\phi}_{\Delta}(\vec{\xi}_4,\vec{\xi}_5,\mu_{\Delta}^{B})]$ and $[\hat{\phi}_{\rm C_8}(\vec{\xi}_1,\vec{\xi}_2,\mu_{\rm C_8}^{A})\hat{\phi}_{\rm C_8}(\vec{\xi}_4,\vec{\xi}_5,\mu_{\rm C_8}^{B})]$, the two components in Eq. (A7) are orthogonal to each other. These two effective relative wave functions are also called channel wave function in nuclear physics and hadronization in hadron physics [53–55].

Finally, for easily carrying out analytic derivation in later calculations, the effective relative wave functions $\chi_{\Delta\Delta(C_8C_8)}$ can also be expended by a set of Gaussian functions

$$\chi_{\Delta\Delta(\rm C_8C_8)}(r)=\sum_{m=1}^{4}\frac{c_m^{\Delta\Delta(\rm C_8C_8)}}{\sqrt{4\pi}}\exp\left(-\frac{r^2}{2(b_m^{\Delta\Delta(\rm C_8C_8)})^2}\right), \tag{A8}$$

where $c_m^{\Delta\Delta(\rm C_8C_8)}$ and $b_m^{\Delta\Delta(\rm C_8C_8)}$ can be determined in the curve fitting process.

[1] M. Bashkanov *et al.*, Double-Pionic Fusion of Nuclear Systems and the "ABC" Effect: Approaching a Puzzle by Exclusive and Kinematically Complete Measurements, Phys. Rev. Lett. **102**, 052301 (2009).

[2] P. Adlarson *et al.* (WASA-at-COSY Collaboration), ABC Effect in Basic Double-Pionic Fusion—Observation of a new resonance?, Phys. Rev. Lett. **106**, 242302 (2011).

[3] P. Adlarson *et al.* (WASA-at-COSY Collaboration), Isospin decomposition of the basic double-pionic fusion in the region of the ABC effect, Phys. Lett. B **721**, 229 (2013).

[4] P. Adlarson *et al.* (WASA-at-COSY Collaboration), Evidence for a New Resonance from Polarized Neutron-Proton Scattering, Phys. Rev. Lett. **112**, 202301 (2014).

[5] H. X. Chen, W. Chen, X. Liu, and S. L. Zhu, The hidden-charm pentaquark and tetraquark states, Phys. Rep. **639**, 1 (2016).

[6] F. K. Guo, C. Hanhart, U. G. Meissner, Q. Wang, Q. Zhao, and B. S. Zou, Hadronic molecules, Rev. Mod. Phys. **90**, 015004 (2018).

[7] Y. Dong, A. Faessler, and V. E. Lyubovitskij, Description of heavy exotic resonances as molecular states using phenomenological Lagrangians, Prog. Part. Nucl. Phys. **94**, 282 (2017).

[8] X. Q. Yuan, Z. Y. Zhang, Y. W. Yu, and P. N. Shen, $\Delta\Delta$ dibaryon structure in chiral $SU(3)$ quark model, Phys. Rev. C **60**, 045203 (1999).

[9] M. Bashkanov, S. J. Brodsky, and H. Clement, Novel six-quark hidden-color dibaryon states in QCD, Phys. Lett. B **727**, 438 (2013).

[10] F. Huang, Z. Y. Zhang, P. N. Shen, and W. L. Wang, Is d^* a candidate for a hexaquark-dominated exotic state?, Chin. Phys. C **39**, 071001 (2015).

[11] F. Huang, P. N. Shen, Y. B. Dong, and Z. Y. Zhang, Understanding the structure of $d^*(2380)$ in chiral quark model, Sci. China Phys. Mech. Astron. **59**, 622002 (2016), and references therein.

[12] Y. Dong, P. Shen, F. Huang, and Z. Zhang, Theoretical study of the $d^*(2380) \to d\pi\pi$ decay width, Phys. Rev. C **91**, 064002 (2015).

[13] Y. Dong, F. Huang, P. Shen, and Z. Zhang, Decay width of $d^*(2380) \to NN\pi\pi$ processes, Phys. Rev. C **94**, 014003 (2016).

[14] Y. Dong, F. Huang, P. Shen, and Z. Zhang, On the decays of $d^*(2380)$ in a constituent chiral quark model, Chin. Phys. C **41**, 101001 (2017).

[15] Y. Dong, F. Huang, P. Shen, and Z. Zhang, Decay width of the $d^*(2380) \to NN\pi$ process in a chiral constituent quark model, Phys. Lett. B **769**, 223 (2017).

[16] The WASA-at-COSY Collaboration, Isoscalar single-pion production in the region of Roper and $d^*(2380)$ resonances, Phys. Lett. B **774**, 599 (2017).

[17] A. Gal, The $d^*(2380)$ dibaryon resonance width and decay branching ratios, Phys. Lett. B **769**, 436 (2017).

[18] A. Gal and H. Garcilazo, Three Body Calculation of the $\Delta\Delta$ Dibaryon Candidate $D_{03}(2370)$, Phys. Rev. Lett. **111**, 172301 (2013).

[19] A. Gal and H. Garcilazo, Three-body model calculations of $N\Delta$ and $\Delta\Delta$ dibaryon resonances, Nucl. Phys. **A928**, 73 (2014).

[20] M. N. Platonova and V. I. Kukulin, ABC effect as a signal of chiral symmetry restoration in hadronic collisions, Phys. Rev. C **87**, 025202 (2013); , Hidden dibaryons in one- and two-pion production in NN collisions, Nucl. Phys. **A946**, 117 (2016).

[21] F. Gross, G. Ramalho, and M. T. Pena, A pure S-wave covariant model for the nucleon, Phys. Rev. C **77**, 015202 (2008).

[22] J. P. B. C. de Melo, T. Frederico, E. Pace, S. Pisano, and G. Salme, Time- and spacelike nucleon electromagnetic form factors beyond relativistic constituent quark models, Phys. Lett. B **671**, 153 (2009).

[23] I. C. Cloet, W. Bentz, and A. W. Thomas, Role of diquark correlations and the pion cloud in nucleon elastic form factors, Phys. Rev. C **90**, 045202 (2014).

[24] W. R. B. de Arujo, J. P. B. C. de Melo, and K. Tsushima, Study of the in-medium nucleon electromagnetic form factors using a light-front nucleon wave function combined with the quark-meson coupling model, Nucl. Phys. **A970**, 325 (2018).

[25] F. Gross, Electromagnetic structure of the deuteron: Review of recent theoretical and experimental results, Eur. Phys. J. A **17**, 407 (2003).

[26] F. Gross and R. A. Gilman, The deuteron: A mini review, AIP Conf. Proc. **603**, 55 (2001).

[27] R. A. Gilman and F. Gross, Electromagnetic structure of the deuteron, J. Phys. G **28**, R37 (2002).

[28] M. Garcon and J. W. Van Orden, The deuteron: Structure and form-factors, Adv. Nucl. Phys. **26**, 293 (2001).

[29] B. D. Sun and Y. B. Dong, Deuteron electromagnetic form factors with the light-front approach, Chin. Phys. C **41**, 013102 (2017).

[30] Y. B. Dong, A. Faessler, T. Gutsche, and V. E. Lyubovitskij, Phenomenological Lagrangian approach to the electromagnetic deuteron form factors, Phys. Rev. C **78**, 035205 (2008).

[31] C. Y. Liang and Y. B. Dong, Deuteron form factors in a phenomenological approach, Chin. Phys. C **39**, 104104 (2015).

[32] A. F. Krutov, R. G. Polezhaev, and V. E. Troitsky, Magnetic moment of the ρ meson in instant-form relativistic quantum mechanics, Phys. Rev. D **97**, 033007 (2018).

[33] A. F. Krutov, R. G. Polezhaev, and V. E. Troitsky, The radius of the rho meson determined from its decay constant, Phys. Rev. D **93**, 036007 (2016).

[34] H. M. Choi and C. R. Ji, Electromagnetic structure of the rho meson in the light front quark model, Phys. Rev. D **70**, 053015 (2004).

[35] J. P. B. C. de Melo and T. Frederico, Covariant and light front approaches to the rho meson electromagnetic form-factors, Phys. Rev. C **55**, 2043 (1997).

[36] D. G. Gudino and G. T. Sanchez, Finite width induced modification to the electromagnetic form factors of spin-1 particles, Phys. Rev. D **81**, 073006 (2010).

[37] V. Simonis, Magnetic properties of ground-state mesons, Eur. Phys. J. A **52**, 90 (2016).

[38] B. D. Sun and Y. B. Dong, ρ meson unpolarized generalized parton distributions with a light-front constituent quark model, Phys. Rev. D **96**, 036019 (2017).

[39] Y. Dong, F. Huang, P. Shen, and Z. Zhang, Charge distribution of d $*$ (2380), Phys. Rev. D **96**, 094001 (2017).
[40] Y. W. Yu, Z. Y. Zhang, P. N. Shen, and L. R. Dai, Quark quark potential from chiral symmetry, Phys. Rev. C **52**, 3393 (1995).
[41] Z. Y. Zhang, Y. W. Yu, P. N. Shen, L. R. Dai, A. Faessler, and U. Straub, Hyperon nucleon interactions in a chiral SU(3) quark model, Nucl. Phys. **A625**, 59 (1997).
[42] L. R. Dai, Z. Y. Zhang, Y. W. Yu, and P. Wang, NN interactions in the extended chiral $SU(3)$ quark model, Nucl. Phys. **A727**, 321 (2003).
[43] P. N. Shen, Z. Y. Zhang, Y. W. Yu, and S. Yang, H-dihyperon in quark cluster model, J. Phys. G **25**, 1807 (1999).
[44] Q. B. Li, P. N. Shen, Z. Y. Zhang, and Y. W. Yu, Dibaryon systems in chiral $SU(3)$ quark model, Nucl. Phys. **A683**, 487 (2001).
[45] K. Wildermuth and Y. C. Tang, *A Unified Theory of the Nucleus* (Academic Press, New York, 1977).
[46] M. Oka and K. Yazaki, Short range part of baryon baryon interaction in a quark model. 2. Numerical results for S-wave, Prog. Theor. Phys. **66**, 572 (1981).
[47] A. Faessler, F. Fernandez, G. Lubeck, and K. Shimizu, The nucleon nucleon interaction and the role of the (42) orbital six quark symmetry, Nucl. Phys. **A402**, 555 (1983).
[48] M. Lacombe, B. Loiseau, R. Vinh Mau, P. Demetriou, J. P. B. C. de Melo, and C. Semay, Testing the quark cluster model in nucleon-nucleon scattering, Phys. Rev. C **65**, 034004 (2002).
[49] A. Faessler, Quark model and the nucleon-nucleon interaction, Prog. Part. Nucl. Phys. **11**, 171 (1984); The short range nucleon-nucleon repulsion and the quark model, Prog. Part. Nucl. Phys.**13**, 253 (1985); Interaction between two baryons and the six quark model, Prog. Part. Nucl. Phys.**20**, 151 (1988).
[50] M. Oka, and K. Yazaki, in *Quarks and Nuclei*, edited by W. Weise (World-Scientific, Singapore, 1984), p. 489.
[51] K. Shimizu, Study of baryon baryon interactions and nuclear properties in the quark cluster model, Rep. Prog. Phys. **52**, 1 (1989).
[52] Y. Yamauchi, K. Tsushima, and A. Faessler, Explicit form of the effective N N potential from the quark cluster model, Few-Body Syst. **12**, 69 (1992).
[53] A. M. Kusainov, V. G. Neudatchin, and I. T. Obukhovsky, Projection of the six-quark wave function onto the NN channel and the problem of the repulsive core in the NN interaction, Phys. Rev. C **44**, 2343 (1991).
[54] L. Ya. Glozman, V. G. Neudatchin, and I. T. Obukhovsky, Exclusive process $^2\mathbf{H}(e, e\prime p)\mathbf{N}^*$ as a tool for investigation of the quark structure of the deuteron, Phys. Rev. C **48**, 389 (1993).
[55] Fl. Stancu, S. Pepin, and L. Ya. Glozman, Nucleon-nucleon interaction in a chiral constituent quark model, Phys. Rev. C **56**, 2779 (1997).
[56] D. Spehler and S. F. Novaes, Helicity wave functions for massless and massive spin-2 particles, Phys. Rev. D **44** (1991) 3990.
[57] T. M. Aliev, K. Azizi, and M. Savci, Heavy χ_{Q_2} tensor mesons in QCD, Phys. Lett. B **690** (2010) 164.
[58] C. Lorce, Electromagnetic properties for arbitrary spin particles. Part 1. Electromagnetic current and multipole decomposition, arXiv:0901.4199.
[59] C. Lorce, Electromagnetic properties for arbitrary spin particles: Natural electromagnetic moments from light-cone arguments, Phys. Rev. D **79**, 113011 (2009).
[60] A. Afanasev, V. D. Afanasev, and S. V. Trubnikov, Magnetic radius of the deuteron, arXiv:nucl-th/9808047.
[61] S. Capstick, Photoproduction amplitudes of P(11) and P(33) baryon resonances in the quark model, Phys. Rev. D **46**, 1965 (1992).
[62] S. Capstick, Photoproduction and electroproduction of nonstrange baryon resonances in the relativized quark model, Phys. Rev. D **46**, 2864 (1992).
[63] P. N. Shen, Y. B. Dong, Z. Y. Zhang, Y. W. Yu, and T.-S. H. Lee, $E2/M1$ ratio of the $\Delta \leftrightarrow \gamma N$ transition within the chiral constituent quark model, Phys. Rev. C **55**, 2024 (1997).
[64] M. Bashkanov (private communication).